International Journal of Mathematical, Engineering and Management Sciences
Vol. 8, No. 4, 560-580, 2023
https://doi.org/10.33889/IJMEMS.2023.8.4.032

Reliability Evaluation and Prediction Method with Small Samples

Hongyan Dui
School of Management,
Zhengzhou University, Zhengzhou, Henan, China.
E-mail: duihongyan@zzu.edu.cn

Xinghui Dong
School of Management,
Zhengzhou University, Zhengzhou, 450001, China.
E-mail: dongxinghui@gs.zzu.edu.cn

Junyong Tao
Laboratory of Science and Technology on Integrated Logistics Support,
College of Intelligence Science and Technology,
National University of Defense Technology,
Changsha, 410073, China.
Corresponding author. taojunyong@nudt.edu.cn

(Received on January 25, 2023; Accepted on March 03, 2023)

Abstract
How to accurately evaluate and predict the degradation state of the components with small samples is a critical and practical problem. To address the problems of unknown degradation state of components, difficulty in obtaining relevant environmental data and small sample size in the field of reliability prediction, a reliability evaluation and prediction method based on Cox model and 1D CNN-BiLSTM model is proposed in this paper. Taking the historical fault data of six components of a typical load-haul-dump (LHD) machine as an example, a reliability evaluation method based on Cox model with small sample size is applied by comparing the reliability evaluation models such as logistic regression (LR) model, support vector machine (SVM) model and back propagation neural network (BPNN) model in a comprehensive manner. On this basis, a reliability prediction method based on one-dimensional convolutional neural network-bi-directional long and short-term memory network (1D CNN-BiLSTM) is applied with the objective of minimizing the prediction error. The applicability as well as the effectiveness of the proposed model is verified by comparing typical time series prediction models such as the autoregressive integrated moving average (ARIMA) model and multiple linear regression (MLR). The experimental results show that the proposed model is valuable for the development of reliability plans and for the implementation of reliability maintenance activities.

Keywords- Reliability evaluation, Cox model, Logistic regression model, Reliability prediction.

ACRONYMS

1D CNN-BiLSTM	One-Dimensional Convolutional Neural Network-Bi-Directional Long and Short-Term Memory Network
ARIMA	Autoregressive Integrated Moving Average
AUC	Area Under the Roc Curve
BiLSTM	Bi-Directional Long and Short-Term Memory Network
BPNN	Back Propagation Neural Network
CNN	Convolutional Neural Network
FN	False Negative
FP	False Positive
FPR	False Positive Rate
LHD	Load-Haul-Dump
LR	Logistic Regression
MAPE	Mean Absolute Percentage Error
MLR	Multiple Linear Regression
PHM	Proportional Hazards Model
RMSE	Root Mean Square Error
ROC	Receiver Operating Characteristic
SVM	Support Vector Machine
TN	Ture Negative
TP	Ture Positive
TPR	True Positive Rate

1. Introduction

With the advent of Industry 4.0, modern machinery and equipment are becoming more and more automated, system functions are becoming richer, and the working environment is more complex. The requirements for safety and reliability of equipment operation are increasing, and system reliability has become one of the important issues of concern in the industrial field. In system reliability theory, systems are divided into two categories: repairable and non-repairable. A non-repairable system is a system that cannot be repaired after a fault. A repairable system is a system that can be repaired after a fault. In the whole life cycle, repairable systems go through an iterative process of operation, analysis and repair (Xing et al., 2002, 2004; Peng et al., 2017). Repairable systems can be found everywhere in production life. And the earliest area of reliability research is the maintenance problem of machines and equipment. The problem of system maintenance has a very wide range of applications in real life. For example, when a component of a car fails, the first consideration should be the repair of the relevant component rather than its replacement. In the maintenance problem, the traditional corrective maintenance and periodic maintenance strategies can no longer meet the needs of daily industrial production and management. For some large transportation tools as well as military strategic equipment, a fault can lead to serious catastrophic accidents. Maintenance strategies have gradually evolved from restorative strategies to preventive maintenance (Dui et al., 2022a) and further to intelligent predictive maintenance (Paul et al., 2022). Therefore, it is essential to accurately evaluate and predict the reliability of complex systems and their components that are subject to high reliability requirements (Dui et al., 2021).

Reliability is the probability that a component performs a specified function under specified conditions and within a specified time. Therefore, the estimation of component reliability is essentially an analysis of component degradation trends from a probabilistic point of view. A lot of work has been done in existing studies to evaluate and improve the reliability of repairable components and systems. For repairable components, considering the impact of the transition rate group between different component states on the probability distribution of the component, Si et al. (2013) extended the composite importance metric to estimate the impact of a component that stays in certain states on the performance of the overall multi-state system. And considering the cost constraints of preventive maintenance, Wu and Coolen (2013) proposed a new cost-based importance measure that considers the cost incurred in maintaining a system and its components over a limited time horizon. In order to perform both corrective maintenance of the faulty components and preventive maintenance of the operational components on a repairable system, Dui et al. (2019) proposed an extended joint integrated importance metric to effectively guide the selection of components with the aim of maximizing the benefits of system performance. Chen et al. (2021) identified weak or vulnerable components of a system by modeling the reliability of a pod slewing system and performing component importance analysis using the integrated importance metric and Griffith importance metric. Considering the differences and interdependencies among components, Zhang et al. (2022) analyzed component maintenance strategies to effectively restore system performance to improve system reliability. Wei et al. (2022) incorporated the side effects of degradation processes into state-based preventive maintenance optimization, based on which a continuous-time discrete-state Markov chain model was developed to describe the individual component's degradation stochastic process. Considering that the maintenance cost can vary for different maintenance policies, Dui et al. (2022b) proposed some preventive maintenance measures for components to improve the reliability of the system considering the maintenance effectiveness. For repairable systems, based on the relationship between cost and reliability, Si et al. (2019) proposed a generalized Birnbaum importance metric to quantify the contribution of individual components to system reliability improvement by considering reliability range, manufacturing complexity, and technical feasibility. Levitin et al. (2020) proposed an efficient analytical modeling approach for analyzing the reliability of k-out-of-n phased task systems. Garg (2021) determined a bi-objective reliability-cost problem for a series-parallel system by using an interactive approach. Yang et al. (2022) addressed the problem of reliability evaluation of multi-state systems with apparent uncertainty based on multi-valued decision diagrams by combining interval theory and fuzzy set theory. For complex mechatronic systems with hierarchical, nonlinear, dependent, uncertain and stochastic properties, Chen et al. (2023) used the Wiener process model to describe the continuous time degradation process and developed the copula hierarchical Bayesian network for reliability evaluation. However, reliability evaluation of components often requires a large number of fault samples, which are used to construct probability distribution functions for the lifetime of the components. In real life, due to cost as well as time and other external factors, the collection of fault samples is not easy, which leads to large errors between the reliability evaluation and the actual situation. The traditional methods of reliability evaluation are not applicable in the case of small samples. In response to the shortcomings of the traditional reliability evaluation methods, a data-driven reliability evaluation method has been proposed (Álvarez et al., 2021; Sharma and Rai, 2021). However, how to make an accurate evaluation of component reliability based on limited fault data is still one of the challenges in existing research.

A large number of methods have been proposed in reliability prediction. These reliability prediction methods can be broadly classified into the following four categories: model-based methods, data-based methods, expert knowledge-based methods, and fusion-based methods (Djeziri et al., 2019). Of these, model-based reliability prediction methods require that there are mathematical models about the system that are known in order to predict component reliability based on the intrinsic mechanisms of failure occurrence as well as the root cause (Chopra and Ram, 2019; Inoue and Yamada, 2020). The data-based reliability prediction method is a direct prediction method of component reliability metrics based on the data collected from the historical operation of the component by means of machine learning and other techniques (Begum and Dohi, 2018; Li et al., 2022). Expert knowledge-based reliability prediction methods, on the other hand, mainly rely on experts in related fields to predict component reliability by building an expert knowledge base and a historical fault database (Podofillini et al., 2023). The fusion-based reliability prediction method combines the three methods mentioned above to make a comprehensive prediction of the trend of component reliability. In recent years, data-based methods have become the focus of research in reliability prediction methods due to their efficiency and practicality. For example, Begum and Dohi, (2018) used a three-layer perceptron neural network with multiple outputs to transform the underlying software fault count data into Gaussian data via the well-known Box-Cox power transformation. The neural network is then used to predict the optimal software release time. Gaonkar et al. (2021) proposed a possibility method for calculating travel time reliability for any type of transportation vehicle under fuzzy type of data. Küçüker and Yet (2022) proposed a Bayesian network (BN) modeling framework that systematically combines design lifetime estimates, operational data, and expert judgment for reliability prediction of aircraft subsystems. Li et al. (2022) proposed an attention-based encoder-decoder recurrent neural networks (RNN) called EDRNN to predict the number of software failures. Existing studies have proposed different data-driven methods for the problem of reliability prediction. However, methods for data prediction are often based on sufficient amount of data. How to make accurate prediction of reliability trends based on the limited historical operational data of components is a challenge in existing studies.

Besides, in engineering practice, the fault of a system does not only depend on its own lifetime, but is also influenced by external covariates such as temperature and humidity as well as internal covariates such as wear, aging and corrosion. In real life, all the covariates associated with a system fault are often difficult to measure. For example, a light bulb and the lampholder to which it is attached is a typical repairable system. And when engineers record historical repair information for a light bulb, they are more concerned with the time of each of its faults. In order to make the model widely applicable, this paper combines the characteristics of repairable systems and uses the time point of each fault as a covariate to characterize the reliability of the component. For example, the age of a light bulb is calculated from the moment it starts working to the moment it fails, which is defined here as the local age, while the age of the whole repairable system is defined as the global age.

In this paper, local age and global age are used as covariates to characterize the reliability of components, and a reliability evaluation and prediction model based on Cox model and 1D CNN-BiLSTM model is proposed. Firstly, the evaluation performances of LR, SVM and BPNN are compared comprehensively by combining the characteristics of repairable systems on a small sample of historical fault data of a typical LHD machine. A fault time series evaluation method based on Cox model is applied. Finally, with the goal of minimizing the prediction error, a reliability prediction method based on 1D CNN-BiLSTM is proposed. The applicability as well as the effectiveness of the proposed model is verified by comparing typical time series prediction models such as ARIMA and MLR. Overall, the framework of the proposed model in this paper is shown in Figure 1.

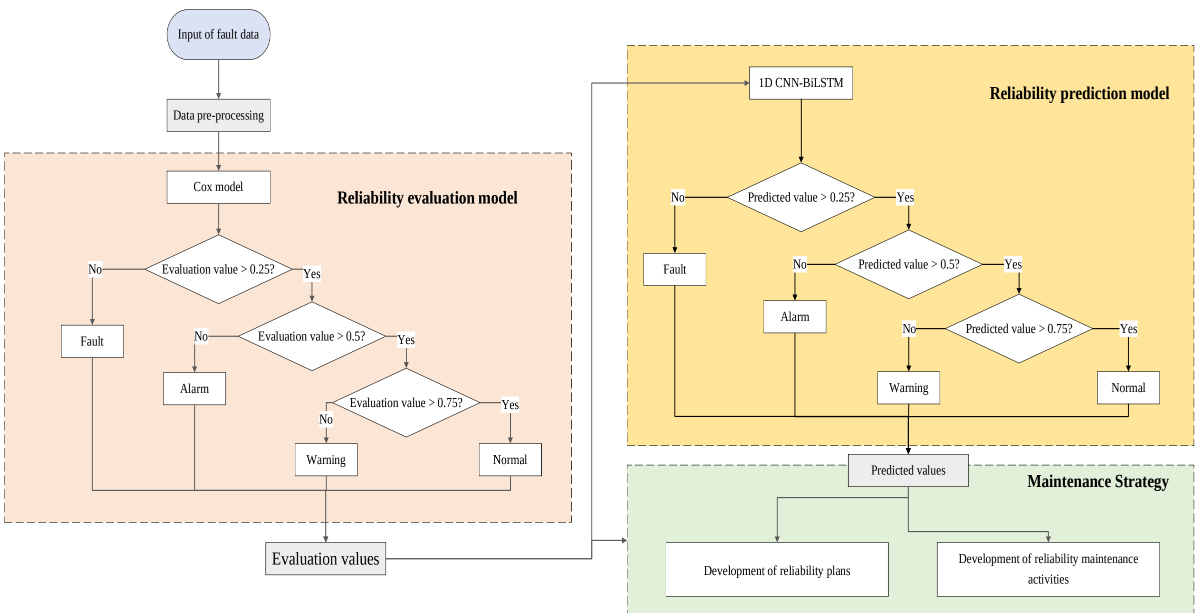

Figure 1. Basic framework of the proposed model.

The rest of the paper is organized as follows. Section 2 presents the classical models used for reliability evaluation, with Cox, LR, SVM, and BPNN being included. Section 3 proposes a reliability prediction model based on 1D CNN-BiLSTM. The historical fault data of six components of LHD are used as examples in Section 4 to illustrate the generality as well as the effectiveness of the proposed method. Finally, the full paper is concluded and future perspectives are given in Section 5.

2. Reliability Evaluation Model

The more common models for evaluating the reliability of components in existing studies are mainly the Cox model, LR, SVM, and BPNN. However, when the sample size of component faults is small (usually in the sense that the number of fault samples is less than 100), there seems to be no clear definition of which model should be used to evaluate the reliability of the component. In this section, these four models are briefly introduced in conjunction with the characteristics of reliability evaluation. A comparison of the performance between these models will be given in Section 4.

2.1 Cox Model

Cox model is also known as proportional hazards model (PHM). It is a semi-parametric regression model proposed by Cox in 1972 to effectively quantify the effects of covariates to represent failure rates (Cox, 1972). The Cox model does not take into account the distribution of component survival times and allows time-dependent variables to be used as predictor variables. The Cox model is now increasingly used in component reliability evaluation, and the basic formulation of the Cox model is shown in Equation (1).

$$h\left(t|X_k(t)\right) = h_0(t)\exp\left(\alpha_0^k + \alpha_1^k x_k^1(t) + \alpha_2^k x_k^2(t) + \cdots + \alpha_m^k x_k^m(t)\right) \tag{1}$$

In Equation (1), $h\left(t|X_k(t)\right)$ is the function of fault rate, indicating the probability of fault of the component k in the next time unit. α_m^k is the Cox regression coefficient of the m-th covariate $x_k^m(t)$ of the component k. $h_0(t)$ is the basic fault rate function. Common basic fault rate functions include exponential distribution, logarithmic distribution and Weibull distribution, etc. For unknown parameters in the basic fault rate function, they can be determined by the method of great likelihood estimation. After obtaining the parameters in the basic fault rate function, the cumulative proportional fault rate of component k can be obtained as

$$H_K\left(t, X_k(t)\right) = \int_0^t h_K\left(t, X_k(t)\right)dt \tag{2}$$

Meanwhile, the reliability function of component k is obtained as

$$R_k\left(t\middle|X_k(t)\right) = \exp\left(-\int_0^t h_K\left(t, X_k(t)\right)dt\right) \tag{3}$$

2.2 Logistic Regression Model

LR can be used to evaluate the relationship between the reliability metrics of components and the covariates that indicate their operational status. It is based on a set of categorical data to build a regression model between a response variable and one or more explanatory variables (Mudunuru et al., 2020). The role of LR is often underestimated when dealing with small datasets or datasets of events of interest. It is highly flexible in its assumptions and has wide applicability. It has a wide range of applications in many fields. Based on this regression model, some reasonable evaluation can be made for the reliability metrics of components. In LR, each sample *k* corresponds to a working state at time t. The response variable is defined as fault ($Y_k^t = 0$) or not faulted ($Y_k^t = 1$). $X_k(t) = \{x_k^1(t), x_k^2(t), \ldots, x_k^m(t)\}$ represents covariates of component *k*. From the definition of reliability, the reliability function of component *k* at moment *t* is shown in Equation (4).

$$R_k\left(t\middle|X_k(t)\right) = P\left(Y_k^t = 1\middle|X_k(t)\right) = \frac{\exp\left(\theta_0^k + \theta_1^k x_k^1(t) + \theta_2^k x_k^2(t) + \cdots + \theta_m^k x_k^m(t)\right)}{1 + \exp\left(\theta_0^k + \theta_1^k x_k^1(t) + \theta_2^k x_k^2(t) + \cdots + \theta_m^k x_k^m(t)\right)} \tag{4}$$

In Equation (4), θ_m^k represents the logistic regression coefficient of the m-th covariate $x_k^m(t)$ of component *k*. θ_0^k is a constant term greater than 0. At this point, the ratio of the reliability function of component k to the cumulative fault distribution function can be obtained as

$$\frac{R_k\left(t\middle|X_k(t)\right)}{1 - R_k\left(t\middle|X_k(t)\right)} = \exp\left(\theta_0^k + \theta_1^k x_k^1(t) + \theta_2^k x_k^2(t) + \cdots + \theta_m^k x_k^m(t)\right) \tag{5}$$

Considering the non-linear characteristics of LR, the regression coefficients in Equation (5) can be solved by using the maximum likelihood estimation method. The final reliability function of component *k* can be obtained expressed as,

$$R_k\left(t\middle|X_k(t)\right)=\frac{\exp\left(\hat{\theta}_0^k+\hat{\theta}_1^k x_k^1(t)+\hat{\theta}_2^k x_k^2(t)+\cdots+\hat{\theta}_m^k x_k^m(t)\right)}{1+\exp\left(\hat{\theta}_0^k+\hat{\theta}_1^k x_k^1(t)+\hat{\theta}_2^k x_k^2(t)+\cdots+\hat{\theta}_m^k x_k^m(t)\right)} \tag{6}$$

2.3 Support Vector Machine Model

SVM has been widely used in the field of reliability evaluation because of its strong small sample learning capability and generalization ability. The core idea of SVM model lies in maximizing the separation of the two classes of training samples. That is, how to construct a classification hyperplane that maximizes the separation between the two classes of training samples (Li et al., 2003), so as to achieve an effective evaluation of the operational state of the components. The common mapping functions of SVM are linear kernel function, polynomial kernel function and Sigmoid kernel function. Based on experience, the more commonly used and well-performing Gaussian radial basis function is chosen as the kernel function for training in this paper. The expression of the Gaussian radial basis function is as follows.

$$K\left(X_i^k,X_j^k\right)=e^{\frac{-\|x_i^k-x_j^k\|^2}{2\delta_k^2}} \tag{7}$$

In Equation (7), X_i^k represents the training tuple of component k, and δ_k is the parameter of the Gaussian radial basis kernel function of component k. After choosing the kernel function, the performance of the SVM is then mainly affected by two parameters, that is, the penalty factor C_k for misclassified samples and the parameter δ_k of the kernel function. Meanwhile, the following optimization problem need to be solved when training two types of samples i, j in component k, which is shown in Equation (8).

$$min\ \frac{1}{2}\parallel w_k^{ij}\parallel^2+C_k\sum_{t=1}^{l}\xi_t^{ij}.$$

$$s.t.\begin{cases} w_k^{ij}\cdot K\left(X_k(t)\right)+b_k^{ij}\geq 1-\xi_{tk}^{ij},\ Y_k^t=i \\ w_k^{ij}\cdot K\left(X_k(t)\right)+b_k^{ij}\leq -1+\xi_{tk}^{ij},\ Y_k^t=j \\ \xi_{tk}^{ij}\geq 0,\ i,j=1,2,\dots,l \end{cases} \tag{8}$$

In Equation (8), K is the Gaussian radial basis kernel function that maps $X_k(t)$ to a high-dimensional feature space, C_k is the penalty factor of component k, w_k is the weight vector associated with the explanatory variables in the new space of component k, b_k is the estimated bias term of component k, and ξ_{tk}^{ij} is the relaxation variable of component k. Once the weight vector and the deviation term are determined, the operational status of component k can be evaluated. At this point, the reliability evaluation function is shown in Equation (9).

$$R_k\left(t\middle|X_k(t)\right)=P\left(Y_k^t=1\middle|X_k(t)\right)=\frac{1}{1+\exp\left(A_K f_K\left(X_k(t)\right)+B_K\right)} \tag{9}$$

In Equation (9), $f_K\left(X_k(t)\right)$ is the prediction function of component k, and A_K and B_K are the multilayer perceptron coefficients of component k, respectively.

2.4 Back Propagation Neural Network Model

BPNN is a multilayer feedforward neural network which is trained according to the error back propagation algorithm. It is one of the most widely used neural network models in deep learning (Feng et al., 2019). BPNN can be analyzed and deduced from the operational data of the components, which is consequently widely used in the reliability assessment of components.

In terms of structure, BPNN has an input layer, a hidden layer and an output layer. Essentially, the BP algorithm takes the squared error of the network as the objective function and uses the gradient descent method to calculate the minimum value of the objective function. The basic idea of BP is the gradient descent method, which uses the gradient search technique to minimize the mean squared error between the actual output and the desired output of the network. The error function of BPNN is defined as

$$E = \frac{1}{2n_k}\sum_{i=1}^{n_k}\sum_{j=1}^{m_k}(Y_{kij}^t - \hat{Y}_{kij}^t)^2 \tag{10}$$

In Equation (10), n_k represents the dimension of the output vector of component k in the network, and m_k represents the dimension of the input vector of component k in the network. Y_{kij}^t represents the actual value of component k at the *j*-th input vector in the dimension of the *i*-th input vector, and $\hat{Y}_{kij}^t$ represents the output value of component k at the *j*-th input vector in the dimension of the *i*-th input vector. Until the calculated error is less than the set prediction accuracy, the training is finished.

2.5 Performance Comparison of Evaluation Models

Once the model for reliability evaluation has been built, the performance of the model needs to be evaluated. In this paper, the model is trained using the training set and evaluated using the relevant metrics from the test set. For components of repairable systems, if the accuracy of the reliability evaluation model is very low, the model cannot be applied in practice. For this reason, this paper evaluates the performance of the model in terms of the following metrics.

For the problem of reliability evaluation, the loss caused by a fault being misclassified is much greater than the loss caused by a fault not being misclassified. In this paper, we record normal status of components as positive cases and abnormal status as negative cases. Considering that the accuracy rate does not accurately reflect the cost of misclassification, the precision rate as well as the recall rate are introduced into the metrics for evaluating the performance of the model. If all the classification results are represented in a table, it is called the confusion matrix, which is shown in Table 1.

Table 1. Confusion matrix.

Sample	Prediction result	
	Positive	Negative
Positive	Ture Positive (TP)	False Negative (FN)
Negative	False Positive (FP)	Ture Negative (TN)

From the confusion matrix, we can obtain the relevant evaluation metrics. Some of the more commonly used evaluation metrics are shown in Table 2.

It is important to note in particular that reliability evaluation problems often involve multiple classifications. In real life, engineers often classify components into different health states according to the operating status and health of the components. The four health states that are often used are normal, warning, alarm, and fault. For a component with a normal health state, a positive example means that the component has a normal health state, while a negative example includes a component with health states of warning, alarm, or fault. In other words, the evaluation metrics used in this paper can be extended to multi-category problems.

In addition, receiver operating characteristic (ROC) curves are often used to evaluate reliability evaluation models, where the true positive rate (TPR) and false positive rate (FPR) are calculated at different thresholds and plotted as vertical and horizontal coordinates, respectively. The area under the ROC curve is called AUC, and the closer the AUC is to 1, the better the classifier is (Nusinovici et al., 2020). For the multi-classification problem, the AUC is then the average of the different AUC corresponding to the component in different health states. In consideration, the AUC curve, the precision rate and the recall rate are used as the evaluation metrics for the reliability evaluation of components in this paper.

Table 2. Relevant evaluation indicators.

Evaluation metrics	Definition
Accuracy	$\text{ACC} = \frac{TP+TN}{TP+TN+FP+FN}$
Precision	$\text{P} = \frac{TP}{TP+FP}$
Recall	$\text{R} = \frac{TP}{TP+FN}$
$F-Measure$	$F_1 = \frac{2P*R}{P+R}$

3. Reliability Prediction Model

After evaluating the reliability of the components using the reliability evaluation model in Section 2, further prediction of the reliability of the components is needed in order to arrange the maintenance in advance and reduce the economic loss. To address the problems of low accuracy and stability in existing reliability prediction models, a reliability prediction model based on 1D CNN-BiLSTM model is proposed in this paper. In order to fully reflect the characteristics of the time series of the component reliability evaluation, firstly, 1D CNN is used to extract the deep features in the reliability time series. Secondly, the memory function of BiLSTM is used to retain the important information in the deep features in order to make accurate prediction for the reliability of the components.

CNN has the ability of representation learning to pan unclassify the input information according to the hierarchical structure and it has been widely used in image classification (Bisht and Gupta, 2020), and speech recognition (Tiwari and Darji, 2022). 1D CNN, then, is an application of CNN model to the extraction of one-dimensional signals. The 1D CNN selects relevant sequence segments along the time dimension from the time series data for reliability evaluation. Then it performs the same transformation on each sequence segment (Abdeljaber et al., 2018). Similar to the CNN model, the network structure of 1D CNN also contains convolutional layers, pooling layers, and fully connected layers. The basic network structure of 1D CNN is illustrated in Figure 2.

In Figure 2, the input of the convolutional layer of component k is defined as $R_k = [R_k^1, R_k^2, \ldots, R_k^{n_k}]^T$, where R_k^n is the evaluation of the reliability of component k at time n_k. Then the output after this input has been processed by the i_k-th convolution kernel of the convolution layer is given as

$$\bar{R}_{i_k} = f_k\left(R_k \cdot W_{ik}^0 + \gamma_k^0\right) \tag{11}$$

In Equation (11), $f_k(*)$ represents the activation function of component k, that is, the nonlinear mapping capability of the model. W_{ik}^0 represents the coefficient of the *i*-th convolution kernel of component k. γ_k^0 is the bias of the convolution layer. The methods used for the pooling layer of component k mainly include two types of maximum pooling and average pooling, which are calculated as follows

$$P_{k_{max}} = \max[\bar{R}_k(t), \bar{R}_k(t+1), \ldots, \bar{R}_k(t+k)] \tag{12}$$

$$P_{k_{mean}} = \text{mean}[\bar{R}_k(t), \bar{R}_k(t+1), \ldots, \bar{R}_k(t+k)] \tag{13}$$

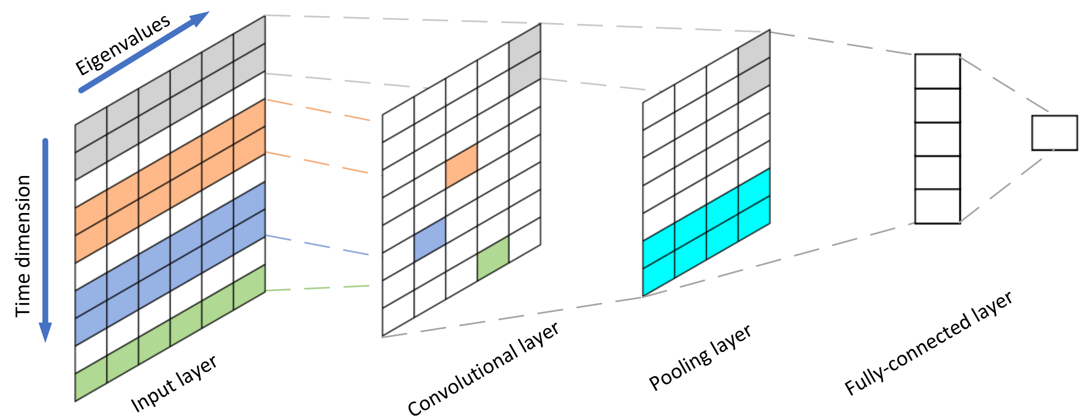

Figure 2. Basic network structure of 1D CNN.

P_k represents the output of the pooling layer for component k. $\bar{R}_k(t)$ is the input to the 1D pooling layer at time t. Before entering the fully connected layer, the original input needs to be flattened. That is, the original multidimensional variables are transformed into one-dimensional variables in order as the input of the fully connected layer of component k. At this point the output of the fully connected layer of component k is given as

$$\hat{R}_k = f_k\left(\bar{P}_k \cdot W_{ik}^1 + \gamma_k^1\right) \tag{14}$$

In Equation (14), $\bar{P}_k$ is the input of the fully connected layer of component k. W_{ik}^1 represents the coefficient of the fully connected layer of component k. γ_k^1 is the bias of the fully connected layer. Finally, the output of the fully connected layer, which is also the output layer of the 1D CNN, can be obtained.

After obtaining the output sequence of the 1D CNN model, the LSTM model can be used for further reliability prediction of the components. The input of the LSTM of component k is the input $h_{k,t}$ at the current moment and the output $h_{k,t-1}$ at the previous moment. The internal structure includes the forgetting gate $F_{k,t}$, the external input gate $I_{k,t}$, and the output gate $O_{k,t}$. The corresponding expressions are given as follows.

$$F_{k,t} = \varepsilon_k\left(W_{F_k} \cdot \left[h_{k,t-1}, \hat{R}_k(t)\right] + b_{F_k}\right) \tag{15}$$
$$I_{k,t} = \varepsilon_k\left(W_{I_k} \cdot \left[h_{k,t-1}, \hat{R}_k(t)\right] + b_{I_k}\right) \tag{16}$$
$$O_{k,t} = \varepsilon_k\left(W_{O_k} \cdot \left[h_{k,t-1}, \hat{R}_k(t)\right] + b_{O_k}\right) \tag{17}$$
$$C_{k,t} = F_{k,t} \cdot C_{k,t-1} + I_{k,t} \cdot \tanh\left(W_{C_k} \cdot \left[h_{k,t-1}, \hat{R}_k(t)\right] + b_{C_k}\right) \tag{18}$$
$$h_{k,t} = O_{k,t} \cdot \tanh\left(C_{k,t}\right) \tag{19}$$

In the above equations, ε_k represents the sigmod function of component k, and $C_{k,t}$ represents the memory cell state of component k. tanh is the hyperbolic tangent function. Considering that the prediction will be jointly affected by the input of multiple moments in front and behind at the same time, BiLSTM is introduced for accurate prediction of the component reliability. BiLSTM mainly has two different hidden layers, forward hidden layer and reverse hidden layer. The forward hidden layer reads the output sequence after the 1D CNN model in the ascending order of the time series. The backward hidden layer reads the output sequence after the 1D CNN model in the descending order of the time series. The forward network output as well as the backward network output are defined as follows.

$$\vec{h}_{k,t} = \overrightarrow{\mathrm{LSTM}}\left(\hat{R}_k(t), \vec{h}_{k,t-1}\right) \tag{20}$$

$$\overleftarrow{h}_{k,t} = \overleftarrow{\mathrm{LSTM}}\left(\hat{R}_k(t), \overleftarrow{h}_{k,t-1}\right) \tag{21}$$

$\vec{h}_{k,t}$ represents the forward hidden state of component k and $\overleftarrow{h}_{k,t}$ represents the backward hidden state of component k. Ultimately, the evaluated value of the reliability of component k can be predicted. In summary, the basic framework diagram of 1D CNN-BiLSTM is shown in Figure 3.

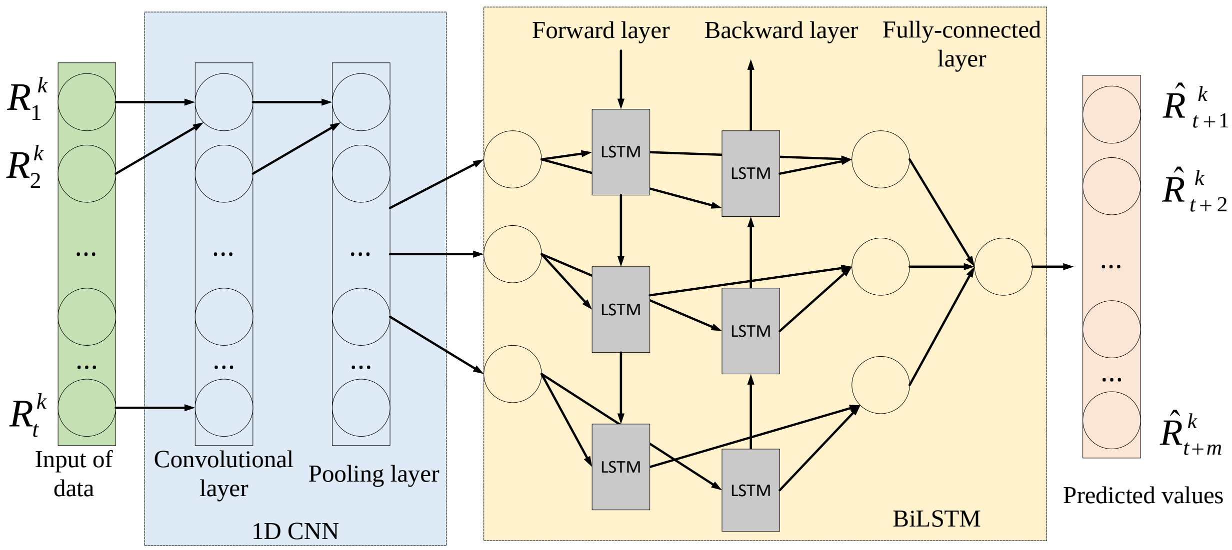

Figure 3. Basic framework diagram of 1D CNN-BiLSTM.

4. Case Study

In order to show the practicality of the proposed model, data related to the faults occurring in six components of LHD (Kumar and Klefsjo, 1992) are used as experimental data for this study. According to the previous description of this paper, local age and global age are used as independent variables to characterize the reliability of the components. Local age is calculated from the moment the component starts working to the moment it fails. The global age is the age of the whole system LHD. Meanwhile, in order to simplify the regression model, reduce the risk of model overfitting, improve the accuracy of model prediction, and facilitate managers to arrange maintenance in advance and save cost time, we discretize the duration of the components, for example, the time period from 0 to 1 is represented by 1. Finally, the occurrence or not of the failure of component k is recorded as the dependent variable Y_k^t, with $Y_k^t = 0$ representing the failure of component k at time t and $Y_k^t = 1$ representing the normal operation of component k at time t.

4.1 Correlation between Variables

Before the reliability of the components can be evaluated, the relationships between the variables need to be discussed. If the correlation between independent variables is very high, the variables with correlation need to be retained or eliminated. The correlation between variables can be expressed by the correlation coefficient. Table 3 shows the correlation coefficient matrix between the variables in LHD1.

Table 3. The matrix of correlation coefficients in LHD1.

	Global age	Local age
Global age	1	
Local age	-0.184	1

At the same time, a significant P-value between the two variables of the variables in LHD1 is obtained as 0.222, which is greater than 0.05, justifying that the correlation between the two variables is not significant. Table 4 shows the correlation coefficients between global age and local age in all components of LHD along with the significant P-values. As can be seen from Table 4, the significant P-values among the independent variables in all six data sets are greater than 0.05, and the correlation between global age and local age is not significant. Further analysis can be performed.

Table 4. Correlation coefficients and significant P-values of LHD.

Type	Correlation coefficient between independent variables	significant P-values
LHD1	-0.184	0.222
LHD3	-0.206	0.160
LHD9	-0.196	0.208
LHD11	-0.056	0.681
LHD17	-0.077	0.588
LHD20	-0.121	0.139

4.2 Data Pre-processing

In general, the collected raw data often suffers from missing, irregular format, and non-equilibrium. In machine learning, data pre-processing plays a key role in optimizing the accuracy of classifiers. Therefore, before analyzing the data, data pre-processing such as relevant cleaning and normalization of the raw data should be considered. The paper mainly focuses on the processing of unbalanced data and the partitioning.

The data imbalance phenomenon is widely found in the fields of anomaly detection and fault diagnosis. For example, data imbalance usually occurs in the fault prediction of repairable systems, where far more faults occur than do not occur. Two conditions are usually required to define a dataset as unbalanced, either an imbalance in the number of classes or an imbalance in the cost of misclassification. Usually, the class that has the majority of samples is called the majority class and the other class is called the minority class. Studies have shown that imbalance exists in a dataset when the majority class sample is three or more times larger than the minority class sample (Liang et al., 2020). When there is data imbalance, classification of the data may result in identifying all the sample data as the majority class. The classification accuracy obtained at this point may be 90% or even higher, but this is not meaningful. For fault prediction of repairable systems, misclassification can be more costly.

There are three main approaches to solve the imbalanced data in existing studies, that is, model adaptive, cost-sensitive and data-driven approaches (Guo et al., 2017). Of these, the data-driven techniques are more widely used. Oversampling or undersampling methods are usually used to construct balanced datasets in data-driven. The undersampling technique is more popular than the oversampling technique. Moreover, it is worth noting that the fault occurs in a sequential order, which leads to a strict sequential order in the time of its fault. In this study, the K-means based undersampling technique is used to handle the imbalanced data in the repairable system, and the original order of the original data is not changed. Finally, each dataset is divided into a training set (70%) as well as a test set (30%). The training set is used to construct the model and search for the parameters in the model by cross-validation. The test set is used to evaluate the performance of the model.

4.3 Reliability Evaluation

In order to show the wide applicability of the Cox-based reliability evaluation model, this paper validates the fault data for each of the six different components of LHD. Four different models, Cox, LR, SVM and BPNN, are used as examples to train the training set respectively. The parameters in the training set models are searched by 5-fold cross-validation. The models obtained are finally validated by using test sets.

Before conducting the experiments, the dataset is divided by the categories of the components of the LHD. To justify this operation, statistical experiments are tested on the partitioned dataset. The results of the mean predicted survival curves for LHD obtained from the Cox are presented in Figure 4. As can be seen in Figure 4, the six sets of curves are almost parallel at different time points. The p-value of the log-rank test obtained at the same time is 0.0002, and the results obtained after correction for the BH method are still statistically significant. This indicates that it is reasonable to divide the data set according to the type of components of the LHD. In addition, the discussion of the reliability evaluation results under different components demonstrates to some extent the practicality of the method presented in this paper. Finally, the results of the reliability evaluation based on the Cox are shown in Figure 5. From Figure 5, it can be seen that the cycle of reliability of the component with the change of global age is well demonstrated by the Cox model.

The results of the reliability evaluation of the components based on LR are presented in Figure 6, which shows that the reliability of the components generally tends to decrease as the global age increases. This result indicates that the reliability of the component is actually affected by the operating time of the system.

Meanwhile, the reliability evaluation results based on SVM and the reliability evaluation results based on BPNN are shown in Figure 7 and Figure 8, respectively.

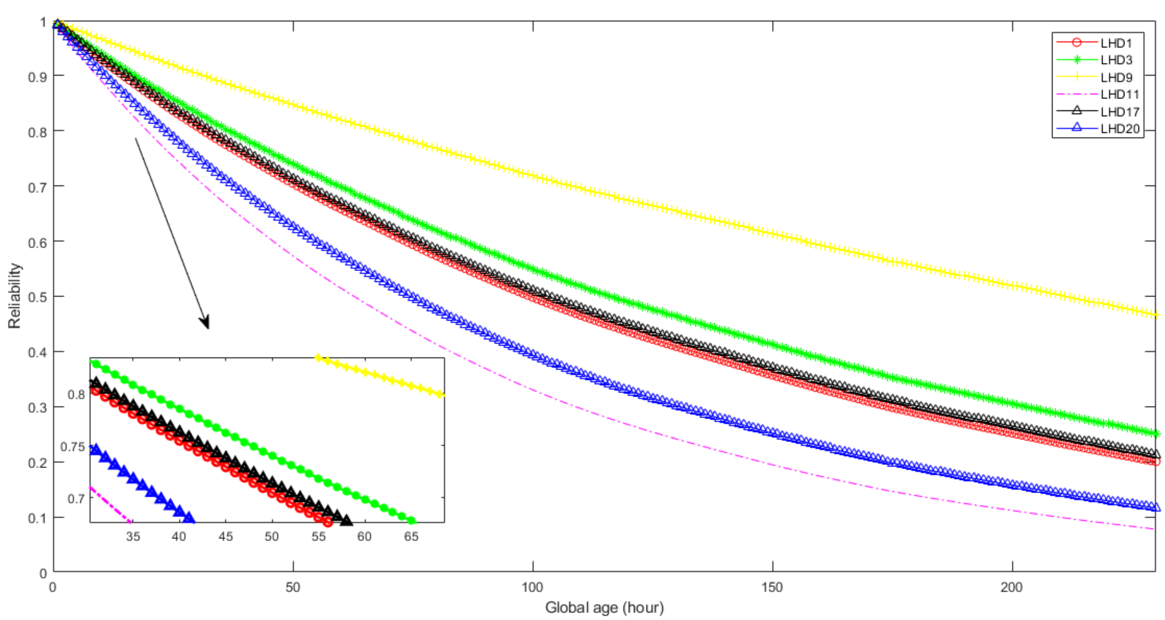

Figure 4. Mean predicted survival curve of LHD.

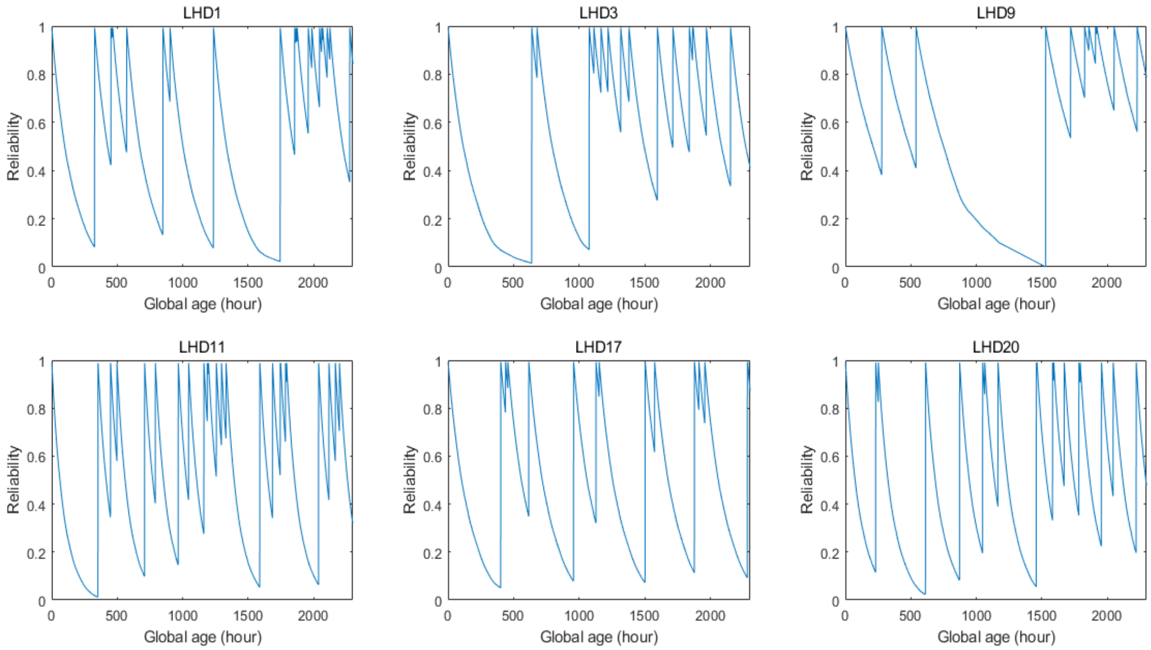

Figure 5. Reliability evaluation results based on Cox model.

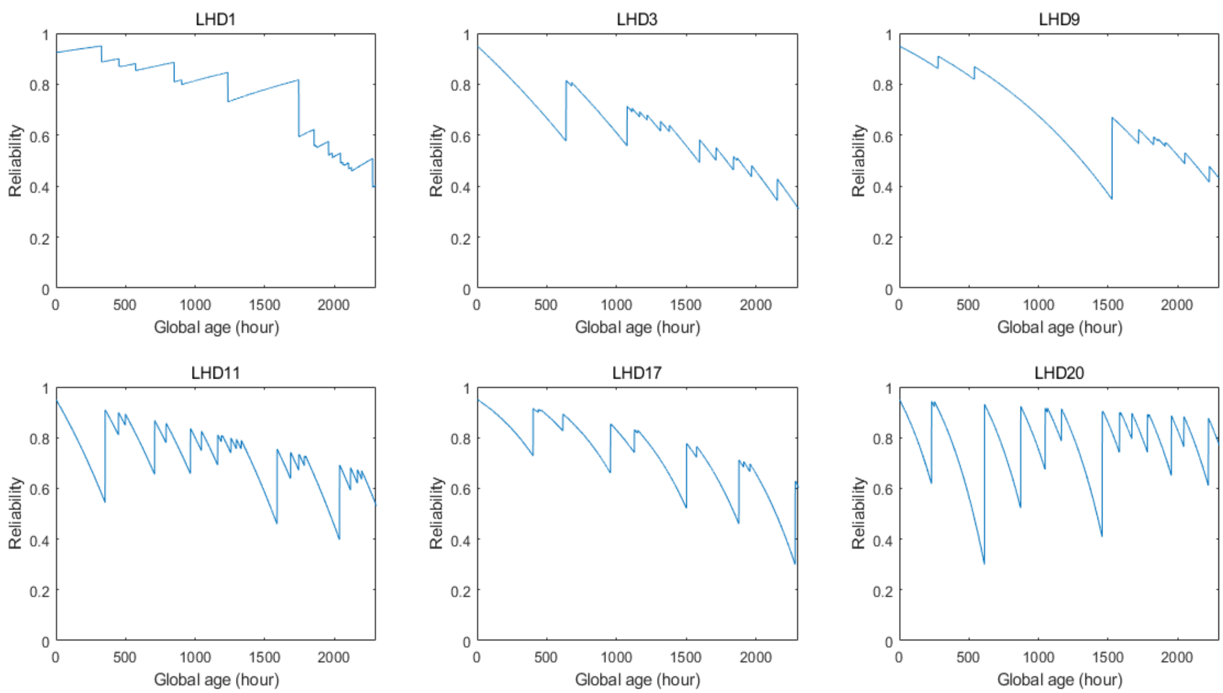

Figure 6. Reliability evaluation results based on LR model.

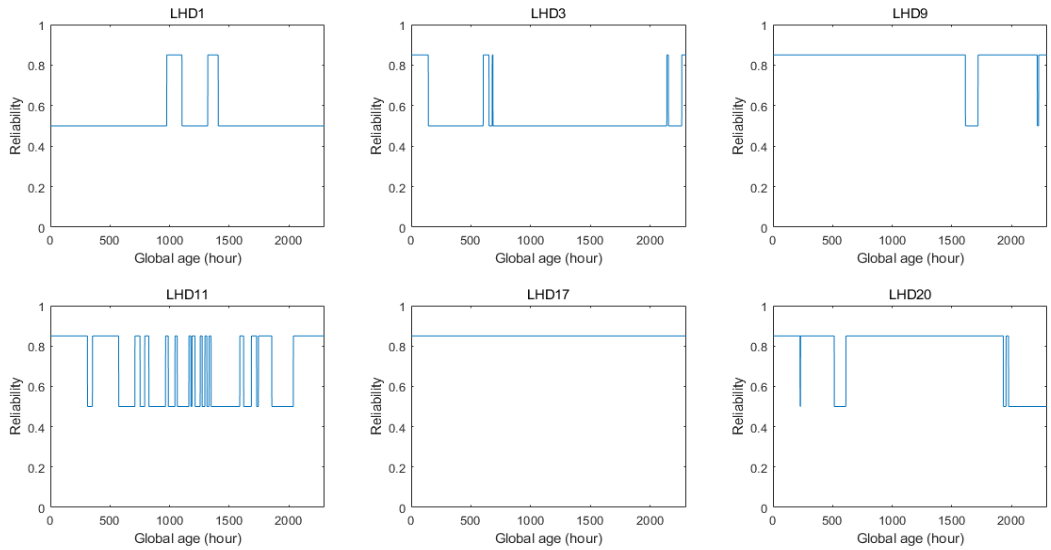

Figure 7. Reliability evaluation results based on SVM model.

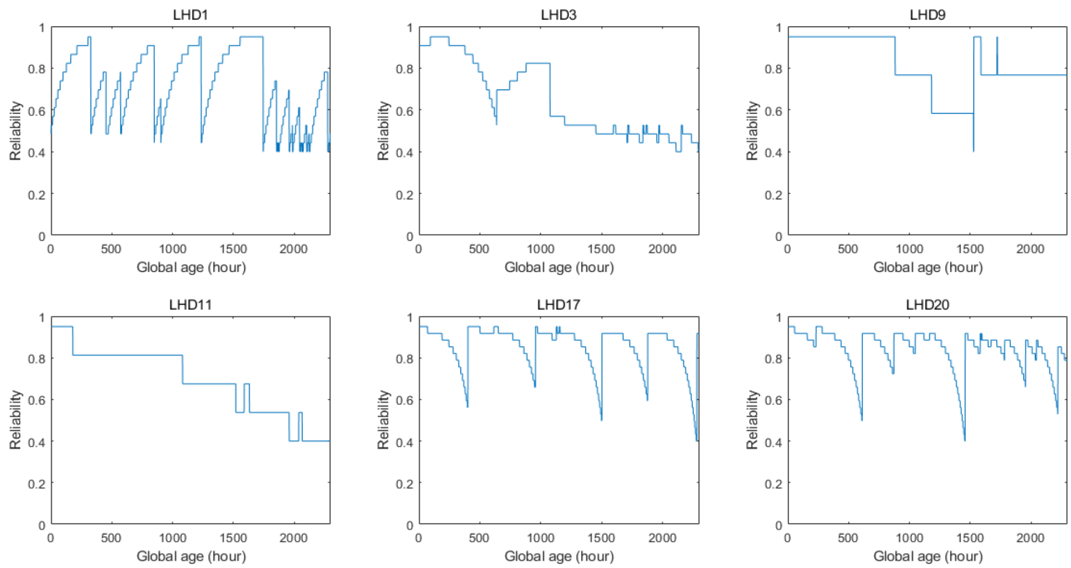

Figure 8. Reliability evaluation results based on BPNN model.

Firstly, it is necessary to classify the operational status of the components of the LHD. Based on practical experience, the health status of the component is classified according to the value of reliability. The reliability evaluation value between 0 and 0.25 indicates a fault of the component, 0.25 to 0.5 indicates an alarm of the component, 0.5 to 0.75 indicates a warning of the component, and 0.75 to 1 indicates the normal of the component. In this paper, the health status of the original data is classified based on the k-means clustering algorithm. The number of clusters is specified as 4. In determining the initial class cluster centroids, the fault data of the components are used as class cluster centroids. The iterative process of the clustering algorithm is stopped until no samples are reclassified. Finally, the experimental results of the test set are obtained as shown in Table 5.

Table 5. Results of reliability evaluation.

Type	Approach	ACC	Recall	Precision	F_1	AUC
LHD1	Cox	0.804	0.783	0.783	0.783	0.792
	LR	0.622	0.609	0.636	0.622	0.681
	SVM	0.500	0.435	0.500	0.465	0.540
	BPNN	0.717	0.609	0.778	0.683	0.737
LHD3	Cox	0.681	0.750	0.667	0.706	0.752
	LR	0.583	0.680	0.586	0.630	0.675
	SVM	0.551	0.583	0.560	0.571	0.520
	BPNN	0.636	0.875	0.618	0.724	0.752
LHD9	Cox	0.709	0.724	0.700	0.712	0.765
	LR	0.655	0.724	0.656	0.688	0.745
	SVM	0.672	0.655	0.678	0.666	0.688
	BPNN	0.672	0.586	0.708	0.641	0.728
LHD11	Cox	0.679	0.679	0.679	0.679	0.723
	LR	0.643	0.750	0.620	0.679	0.691
	SVM	0.554	0.429	0.572	0.490	0.545
	BPNN	0.536	0.714	0.527	0.606	0.575
LHD17	Cox	0.731	0.731	0.731	0.731	0.695
	LR	0.615	0.731	0.594	0.655	0.676
	SVM	0.539	0.580	0.536	0.557	0.500
	BPNN	0.635	0.885	0.590	0.708	0.573
LHD20	Cox	0.652	0.696	0.640	0.667	0.711
	LR	0.674	0.696	0.667	0.681	0.715
	SVM	0.500	0.435	0.500	0.465	0.559
	BPNN	0.609	0.609	0.609	0.609	0.661

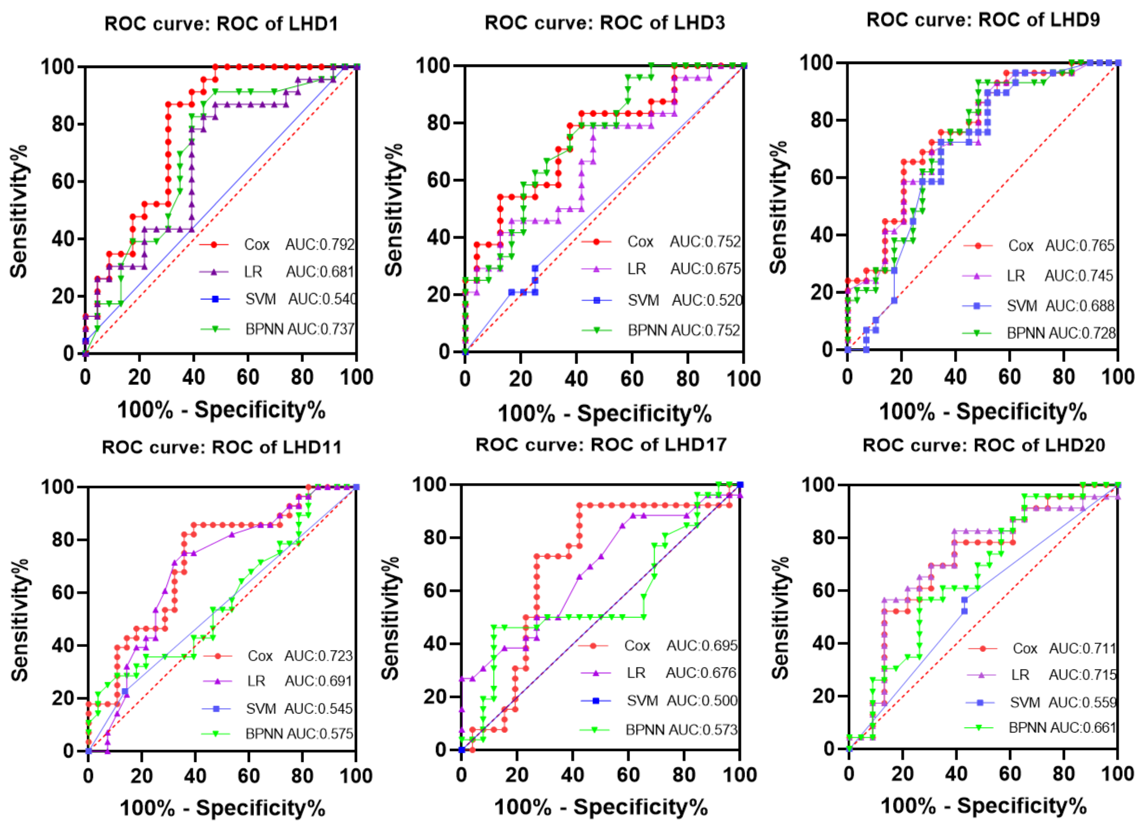

Figure 9. ROC curves for different components of LHD.

For the drawing of ROC curves in the multiclassification, this paper first transforms the multiclassification problem into several dichotomous problems. Considering the characteristics of the samples used in the experiments, the ROC curves of each class derived are arithmetically averaged to obtain the ROC curves of the multiclassification problem, that is, the macro-averaged-ROC curves. Figure 9 shows the ROC curves for the components of the LHD under different models.

As we know, for the state evaluation of repairable systems, the precision rates and the recall rates are more important than the accuracy rates. In practice, the precision rates and the recall rates affect each other, and high precision rates are often accompanied by low recall rates. In order to take into account both precision and recall, we use the summed average F_1 as a metric to evaluate the model evaluation results. The AUC value of the area under the ROC curve is also used as another metric to evaluate the results of the model evaluation. As can be seen from Table 5, the values of Cox model are 0.783, 0.706, 0.712, 0.679, 0.731, and 0.667 respectively for different components of LHD. Cox model has higher values compared to other baseline models. This indicates that Cox model can be applied to repairable systems with small data sets of maintenance histories. The calculation of AUC takes into account both the classification ability of the classifier for positive and negative cases, and it can still give a reasonable evaluation of the classifier in the case of sample imbalance. The closer the value of AUC is to 1, the better the classification ability of the model. In consideration of this, we use the AUC value as another index to evaluate the model evaluation results. As can be seen from Figure 9, Cox model has a higher AUC value, which indicates Cox model can be further applied in the case of data imbalance. Meanwhile, LR model has a relatively high AUC value. Although SVM model is often used to deal with the classification problem of small samples, the classification ability of SVM model is not stable as seen in Figure 9. The classification ability of the BPNN model is also unstable when the sample size is relatively small. The experimental results show that the evaluation performances of the Cox model and the LR model are much better than those of the SVM model and the BPNN model. Of these, the Cox model has the best reliability evaluation performance, and the LR model has the second performance, and both of them have more stable evaluation performance. The performances of the SVM and BPNN reliability evaluation models are more volatile, while the former has a higher risk of misclassification. This also reflects the fact that machine learning algorithms often require sufficiently large sample data. When the sample size is relatively small, the performance of machine learning algorithms will be degraded. Compared with the LR model, the Cox model is able to reflect the dynamic process of the reliability of the components with the working time of the whole system. As a result, the Cox model is further applied to the reliability prediction of LHD components in this paper.

4.4 Reliability Prediction

After the reliability evaluation model of a component is built, the working condition of the component can be monitored in real time. However, the reliability evaluation model does not predict the change trend of the working condition of the component. In order to arrange maintenance in advance and reduce economic losses, this paper proposes a reliability prediction model based on 1D CNN-BiLSTM model to address the problems of low accuracy and stability in the existing reliability prediction models. Firstly, in order to compare the effects of different prediction models more realistically, the dataset of reliability of components obtained based on Cox model is divided into training set (90%) and test set (10%). Secondly, 1D CNN is used to extract the deep features in the reliability time series. Finally, the memory function of BiLSTM is used to retain the important information in the deep features for accurate prediction of the component reliability. Finally, the reliability prediction results are obtained as shown in Figure 10. From Figure 10, it can be seen that the proposed model of reliability prediction can roughly reflect the change trend of the reliability of different components. Meanwhile, the proposed model can accurately predict the working condition of the components in the short term. And from the long-term perspective, the accuracy of the reliability prediction model tends to decrease. In actual production, managers should make adjustments to the production management process based on the proposed reliability prediction model and the historical failure information database, so as to formulate the corresponding reliability plan and maintenance activities in time.

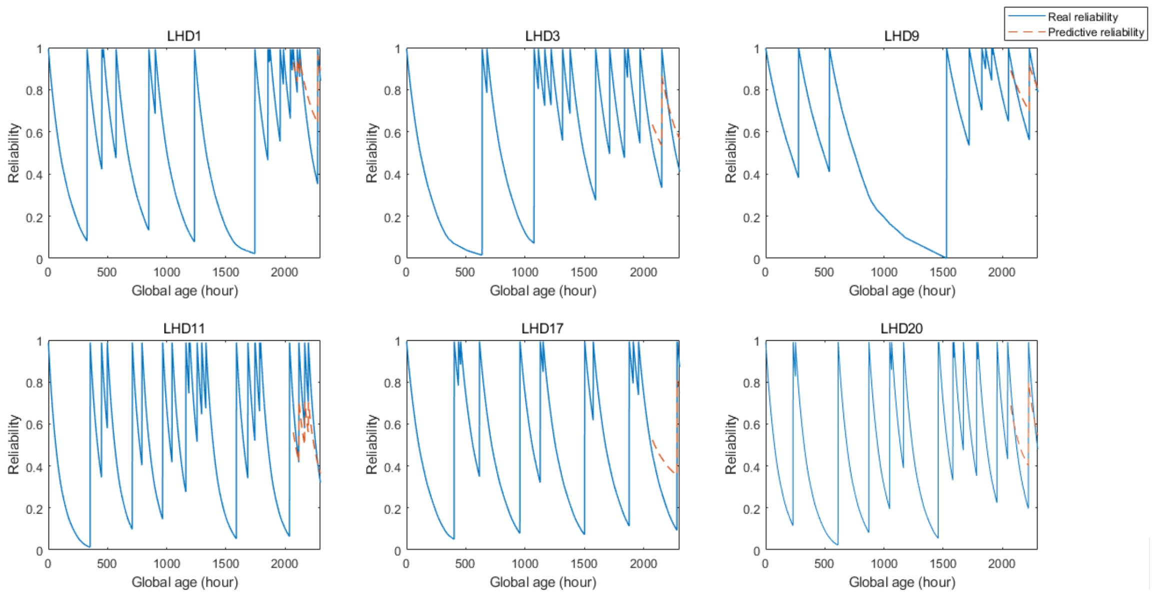

Figure 10. Reliability prediction results based on 1D CNN-BiLSTM model.

In order to further verify the applicability as well as the effectiveness of the models used in this paper, the typical time series prediction models such as ARIMA and MLR are comprehensively compared in this paper, and the root mean square error (RMSE) as well as the mean absolute percentage error (MAPE) are used as the performance metrics of the prediction models (Zhao et al., 2022). In particular, the MLR model for time series prediction is $Y_t^k = a_0^k + a_1^k Y_{t-1}^k + a_2^k Y_{t-2}^k + \cdots + a_{m_k}^k Y_{t-m_k}^k + e^k$. Y_t^k is the predicted value of the reliability of component k at time t. $a_{m_k}^k$ is the bias term of the model and e^k is the error term of the model. m_k is the window length of component k. In this paper, the number of fault data of component k is selected as the value of m_k. Finally, the results of the comparison of the performances between different prediction models are presented in Figure 11.

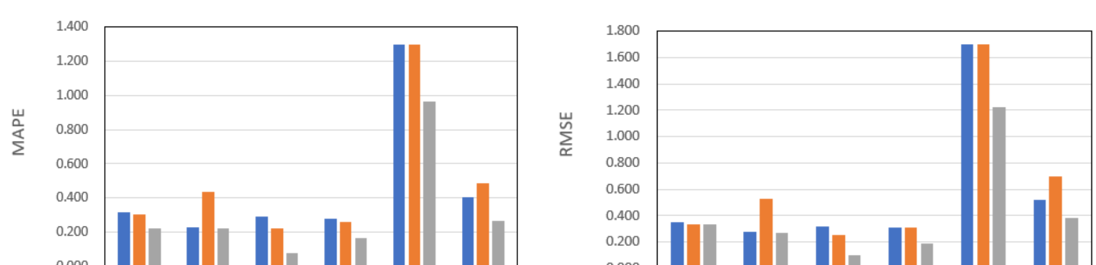

	LHD1	LHD3	LHD9	LHD11	LHD17	LHD20
ARIMA	0.316	0.230	0.292	0.276	1.298	0.403
MLR	0.302	0.436	0.220	0.257	1.298	0.487
1D CNN-BiLSTM	0.222	0.219	0.076	0.164	0.962	0.265

	LHD1	LHD3	LHD9	LHD11	LHD17	LHD20
ARIMA	0.349	0.274	0.314	0.313	1.698	0.516
MLR	0.332	0.530	0.249	0.312	1.698	0.700
1D CNN-BiLSTM	0.330	0.270	0.101	0.184	1.222	0.384

Figure 11. Performance comparison between different prediction models.

As can be seen from Figure 11, RMES and MAPE of the reliability prediction model used in this paper are smaller than those of other models for different LHD components. In other words, compared with other typical time series prediction models, the reliability prediction model used in this paper has higher prediction accuracy and better fitting performance, which can provide a reference for reasonable reliability planning and reliability maintenance activities.

5. Conclusions

To address some problems in the field of reliability prediction, a reliability estimation and prediction method based on Cox model and 1D CNN-BiLSTM model is proposed in this paper. Firstly, taking the historical fault data of six components of a typical load-haul-dump (LHD) machine as an example, a reliability evaluation method based on Cox model is proposed by comparing LR, SVM and BPNN models. On this basis, a reliability prediction method based on 1D CNN-BiLSTM is proposed with the objective of minimizing the prediction error. The applicability as well as the effectiveness of the proposed model is verified by comparing typical time series prediction models such as ARIMA and MLR. The experimental results show that the proposed model is valuable for the development of reliability plans for components of repairable systems with small samples and for the implementation of reliability maintenance activities. When the historical maintenance records of components are relatively few, the Cox model can be considered primarily by engineers to evaluate the reliability of the components. Besides, LR can also be used as a decision aid to evaluate the reliability of components. The reliability prediction results based on the 1D CNN-BiLSTM model at last can be used as a reference.

Of course, the limitations of the model should be taken into account in the industrial production in practice. In order to make the model widely applicable, we have simplified the covariates that affect the occurrence of faults in repairable systems. However, in engineering practice, the fault of a system does not only depend on its own lifetime, but is also affected by external covariates such as temperature and humidity, as well as internal covariates such as wear, aging and corrosion. Managers should fully incorporate the characteristics of the repairable systems maintained and add some covariates related to the Cox-based reliability evaluation model in order to further improve the accuracy of the reliability prediction model. At the same time, as the environment changes, it remains a challenge for the model to autonomously adapt and reconfigure to provide managers with real-time decisions. These efforts will be the focus of further consideration in the future.

Conflict of Interest

The authors confirm that there is no conflict of interest to declare for this publication.

Acknowledgments

The authors gratefully acknowledge the financial support for this research from the National Natural Science Foundation of China (Nos. 72071182, U1904211), the Program for Science & Technology Innovation Talents in Universities of Henan Province (No. 22HASTIT022), the Program for young backbone teachers in Universities of Henan Province (No. 2021GGJS007), and the Key Science and Technology Program of Henan Province (No. 222102520019).

References

Abdeljaber, O., Avci, O., Kiranyaz, M.S., Boashash, B., Sodano, H., & Inman, D.J. (2018). 1-D CNNs for structural damage detection: Verification on a structural health monitoring benchmark data. *Neurocomputing*, *275*, 1308-1317.

Álvarez, M.Á.N., Ibáñez, J.C., & de Mingo, C.S. (2021). Reliability assessment of repairable systems using simple regression models. *International Journal of Mathematical, Engineering and Management Sciences*, *6*(1), 180-192.

Begum, M., & Dohi, T. (2018). Optimal release time estimation of software system using Box-Cox transformation and neural network. *International Journal of Mathematical, Engineering and Management Sciences*, *3*(2), 177-194.

Bisht, M., & Gupta, R. (2020). Multiclass recognition of offline handwritten Devanagari characters using CNN. *International Journal of Mathematical, Engineering and Management Sciences*, *5*(6), 1429-1439.

Chen, L., Gao, Y., Dui, H., & Xing, L. (2021). Importance measure-based maintenance optimization strategy for pod slewing system. *Reliability Engineering & System Safety, 216,* 108001. https://doi.org/10.1016/j.ress.2021.108001.

Chen, R., Zhang, C., Wang, S., Zio, E., Dui, H., & Zhang, Y. (2023). Importance measures for critical components in complex system based on Copula Hierarchical Bayesian Network. *Reliability Engineering & System Safety, 230,* 108883. https://doi.org/10.1016/j.ress.2022.108883.

Chopra, G., & Ram, M. (2019). Reliability measures of two dissimilar units parallel system using Gumbel-Hougaard family copula. *International Journal of Mathematical, Engineering and Management Sciences*, *4*(1), 116-130.

Cox, D.R. (1972). Regression models and life-tables (with discussion). *Journal of the Royal Statistical Society Series B-Statistical Methodology*, *34*, 187-220.

Djeziri, M.A., Benmoussa, S., & Benbouzid, M.E. (2019). Data-driven approach augmented in simulation for robust fault prognosis. *Engineering Applications of Artificial Intelligence*, *86*, 154-164.

Dui, H., Li, S., Xing, L., & Liu, H. (2019). System performance-based joint importance analysis guided maintenance for repairable systems. *Reliability Engineering & System Safety*, *186*, 162-175.

Dui, H., Yang, X., & Fang, Y. (2022a). Evaluation methodology for preventive maintenance in multi-state manufacturing systems considering different costs. *International Journal of Production Research*, 1-16. https://doi.org/10.1080/00207543.2022.2127163.

Dui, H., Zhang, C., Tian, T., & Wu, S. (2022b). Different costs-informed component preventive maintenance with system lifetime changes. *Reliability Engineering & System Safety, 228,* 108755. https://doi.org/10.1016/j.ress.2022.108755.

Dui, H., Zheng, X., Zhao, Q.Q., & Fang, Y. (2021). Preventive maintenance of multiple components for hydraulic tension systems. *Eksploatacja i Niezawodność*, *23*(3), 489-497.

Feng, J., Sun, Q., Li, Z., Sun, Z., Jia, K. (2019). Back-propagation neural network-based reconstruction algorithm for diffuse optical tomography. *Journal of Biomedical Optics*, *24*(5), 1-12.

Gaonkar, R. S. P., Nigalye, A. V., & Pai, S. P. (2021). Possibilistic approach for travel time reliability evaluation. *International Journal of Mathematical, Engineering and Management Sciences*, *6*(1), 223-243.

Garg, H. (2021). Bi-objective reliability-cost interactive optimization model for series-parallel system. *International Journal of Mathematical, Engineering and Management Sciences*, *6*(5), 1331-1344.

Guo, H., Li, Y., Shang, J., Gu, M., Huang, Y., & Gong, B. (2017). Learning from class-imbalanced data: Review of methods and applications. *Expert Systems with Applications*, *73*, 220-239.

Inoue, S., & Yamada, S. (2020). Phase-type modeling approaches for software reliability modeling with debugging process. *International Journal of Mathematical, Engineering and Management Sciences*, *5*(1), 76-82.

Küçüker, F.U., & Yet, B. (2022). Reliability prediction for aircraft fleet operators: A Bayesian network model that combines supplier estimates, maintenance data and expert judgement. *Journal of the Operational Research Society*, 1-12. https://doi.org/10.1080/01605682.2022.2129486.

Kumar, U., & Klefsjö, B. (1992). Reliability analysis of hydraulic systems of LHD machines using the power law process model. *Reliability Engineering & System Safety*, *35*(3), 217-224.

Levitin, G., Finkelstein, M., & Xiang, Y. (2020). Optimal multi-attempt missions with cumulative effect. *Reliability Engineering & System Safety, 203,* 107091. https://doi.org/10.1016/j.ress.2020.107091.

Li, C., Zheng, J., Okamura, H., Dohi, T. (2022). Software reliability prediction through encoder-decoder recurrent neural networks. *International Journal of Mathematical, Engineering and Management Sciences*, *7*(3), 325-340.

Li, S., Kwok, J.T., Zhu, H., & Wang, Y. (2003). Texture classification using the support vector machines. *Pattern Recognition*, *36*(12), 2883-2893.

Liang, X. W., Jiang, A.P., Li, T., Xue, Y.Y., & Wang, G.T. (2020). LR-SMOTE—An improved unbalanced data set oversampling based on K-means and SVM. *Knowledge-Based Systems, 196,* 105845. https://doi.org/10.1016/j.knosys.2020.105845.

Mudunuru, V.R., & Skrzypek, L.A. (2020). A comparison of artificial neural network and decision trees with logistic regression as classification models for breast cancer survival. *International Journal of Mathematical, Engineering and Management Sciences*, *5*(6), 1170-1190.

Nusinovici, S., Tham, Y.C., Yan, M.Y.C., Ting, D.S.W., Li, J., Sabanayagam, C., Wong, T.Y., & Cheng, C.Y. (2020). Logistic regression was as good as machine learning for predicting major chronic diseases. *Journal of Clinical Epidemiology*, *122*, 56-69.

Paul, A.R., Biswas, S., & Mukherjee, M. (2022). Conceptualisation of a novel technique to incorporate artificial intelligence in preventive and predictive maintenance in tandem. *Materials Today: Proceedings*, *66*, 3814-3821.

Peng, Y., Wang, Y., Zi, Y., Tsui, K.L., & Zhang, C. (2017). Dynamic reliability assessment and prediction for repairable systems with interval-censored data. *Reliability Engineering & System Safety*, *159*, 301-309.

Podofillini, L., Reer, B., & Dang, V.N. (2023). A traceable process to develop Bayesian networks from scarce data and expert judgment: A human reliability analysis application. *Reliability Engineering & System Safety, 230,* 108903. https://doi.org/10.1016/j.ress.2022.108903.

Sharma, G., & Rai, R.N. (2021). Age based overhaul policy for multiple repairable systems with imperfect maintenance: case study of Aero engines. *International Journal of Mathematical, Engineering and Management Sciences*, *6*(1), 193-206.

Si, S., Levitin, G., Dui, H., & Sun, S. (2013). Component state-based integrated importance measure for multi-state systems. *Reliability Engineering & System Safety*, *116*, 75-83.

Si, S., Liu, M., Jiang, Z., Jin, T., & Cai, Z. (2019). System reliability allocation and optimization based on generalized Birnbaum importance measure. *IEEE Transactions on Reliability*, *68*(3), 831-843.

Tiwari, P., & Darji, A.D. (2022). A novel S-LDA features for automatic emotion recognition from speech using 1-D CNN. *International Journal of Mathematical, Engineering and Management Sciences*, *7*(1), 49-67.

Wei, S., Nourelfath, M., & Nahas, N. (2022). Condition-based maintenance optimization of degradable systems. *International Journal of Mathematical, Engineering and Management Sciences*, *7*(1), 1-15.

Wu, S., & Coolen, F.P. (2013). A cost-based importance measure for system components: An extension of the Birnbaum importance. *European Journal of Operational Research*, *225*(1), 189-195.

Xing, L., & Dugan, J.B. (2002). Analysis of generalized phased-mission system reliability, performance, and sensitivity. *IEEE Transactions on Reliability*, *51*(2), 199-211.

Xing, L., & Dugan, J.B. (2004). A separable ternary decision diagram based analysis of generalized phased-mission reliability. *IEEE Transactions on Reliability*, *53*(2), 174-184.

Yang, J., Xing, L., Wang, Y., & He, L. (2022). Combinatorial reliability evaluation of multi-state system with epistemic uncertainty. *International Journal of Mathematical, Engineering and Management Sciences*, *7*(3), 312-324.

Zhang, C., Chen, R., Wang, S., Dui, H., & Zhang, Y. (2022). Resilience efficiency importance measure for the selection of a component maintenance strategy to improve system performance recovery. *Reliability Engineering & System Safety*, *217*, 108070. https://doi.org/10.1016/j.ress.2021.108070.

Zhao, D., Zhang, R., Zhang, H., & He, S. (2022). Prediction of global omicron pandemic using ARIMA, MLR, and Prophet models. *Scientific Reports*, *12*, 18138. https://doi.org/10.1038/s41598-022-23154-4.